

Contents lists available at [ScienceDirect](https://www.sciencedirect.com)

Journal of Hazardous Materials

journal homepage: [www.elsevier.com/locate/jhazmat](https://www.elsevier.com/locate/jhazmat)

Research paper

# Multicomponent adsorption of pentavalent As, Sb and P onto iron-coated cork granulates

Ariana M.A. Pintor<sup>\*</sup>, Cátia C. Brandão, Rui A.R. Boaventura, Cidália M.S. Botelho<sup>\*</sup>*Laboratory of Separation and Reaction Engineering – Laboratory of Catalysis and Materials (LSRE-LCM), Departamento de Engenharia Química, Faculdade de Engenharia da Universidade do Porto, Rua Dr. Roberto Frias, 4200-465 Porto, Portugal*

## ARTICLE INFO

Editor: Dr. H. Zaher

## Keywords:

Competitive adsorption  
Pnictogens  
Arsenic  
Antimony  
Phosphorus

## ABSTRACT

The assessment of multicomponent adsorption of pentavalent metalloids is important since they are often found together in groundwaters and mining runoff. For this purpose, adsorption of As(V), Sb(V) and P(V) onto iron-coated cork granulates was studied in binary and ternary systems. Data from equilibrium and kinetic studies revealed that uptake of these contaminants is a multilayer, heterogeneous process well described by Freundlich, extended Freundlich and Elovich models. Most of the observed interactions are competitive and were related to the chemical structure and aqueous behaviour of each anion. Sb(V) adsorption was found to be most impaired and P(V) uptake the least affected by the presence of other pentavalent anions. The aggravation in the reduction of adsorbed amount from binary to ternary solution was more prominent for As(V) than Sb(V). Sb(V) adsorption outweighed that of the other pnictogens in acidic solutions, but in neutral conditions As(V) or P(V) adsorption may predominate instead. P(V) adsorption was the most sensitive to electrolyte addition, namely Ca salts, which may promote precipitation of calcium phosphates. This work provides useful insights regarding the design of adequate adsorption treatment systems for the simultaneous treatment of pentavalent metalloids.

## 1. Introduction

Arsenic and antimony are identified as pollutants of priority interest by both the United States and the European Union, due to their high toxicity to humans and aquatic life. Inorganic arsenic compounds are classified as “carcinogenic to humans”, while antimony ones are “possibly carcinogenic” (Ungureanu et al., 2015). For this reason, their presence in drinking water is strictly limited by very low guideline values, of  $10 \mu\text{g L}^{-1}$  for total As and between  $5 \mu\text{g L}^{-1}$  and  $20 \mu\text{g L}^{-1}$  for total Sb (WHO, 2011).

As and Sb are often encountered simultaneously in the environment, namely in mining fields, as both can be found in sulfide ores (Mirza et al., 2017; Simeonidis et al., 2017). Run-off from tailings and residue piles can cause infiltration of these pollutants to groundwaters, causing a serious environmental problem (Song et al., 2014). Removal of As and Sb from water is, therefore, imperative, for the protection of both human health and water reservoirs.

Remediation of As water contamination has been widely studied using a variety of technologies, including chemical methods, membrane filtration and ion exchange; however, they present disadvantages such as excessive production of sludge or high operation cost. Meanwhile,

adsorption is a practical, easy-to-use, low-cost and low-sludge approach (Baig et al., 2015). Some authors (Sazakli et al., 2014; Ungureanu et al., 2015) suggest that As remediation methods should also be effective for Sb, but others have reported otherwise (Fawcett et al., 2015). This suggestion derives from the fact that As and Sb are chemically similar.

Both As and Sb are metalloids and part of group 15 of the periodic table, characterized by the presence of 5 electrons in the outer valence shell, leading to a common ionic occurrence in the pentavalent oxidation state, often coupled with oxygen as oxyanions. Although these chemical parallels indicate similarities in toxicity, redox behaviour, and environmental fate, they also often lead to competition in water treatment processes. Nevertheless, simultaneous removal of both elements should be a goal, due to their common co-occurrence.

Nitrogen and phosphorus, as more abundant elements from the same periodic table group, may also interfere with As and Sb treatment, namely their uptake by suitable adsorbents. In particular, P is mostly found in the aquatic environment as phosphate, an oxyanion with an identical tetrahedral structure and very similar affinity constants to arsenate (pentavalent As) (Qi and Pichler, 2017). Arsenate’s main toxicity, which is the disruption of phosphorus-mediated biological processes, derives from this characteristic (Giles et al., 2011). On the other hand, phosphate is often applied to soil as a fertilizer, where it may

<sup>\*</sup> Corresponding authors.

E-mail addresses: [ampintor@fe.up.pt](mailto:ampintor@fe.up.pt) (A.M.A. Pintor), [cbotelho@fe.up.pt](mailto:cbotelho@fe.up.pt) (C.M.S. Botelho).

<https://doi.org/10.1016/j.jhazmat.2020.124339>

Received 10 July 2020; Received in revised form 14 October 2020; Accepted 16 October 2020

Available online 22 October 2020

0304-3894/© 2020 Elsevier B.V. All rights reserved.

<b>Nomenclature</b>	$K_F$	Freundlich equilibrium constant ( $\text{mg}^{(1-1/n)} \text{L}^{1/n} \text{g}^{-1}$ )
	$m$	mass of adsorbent (g)
	$n$	dimensionless constant related to adsorbate-adsorbent affinity
<b>List of acronyms</b>	$N_i$	number of measurements for component $i$
<b>FAAS</b>	$N_t$	total number of measurements
<b>GFAAS</b>	$q$	adsorbed amount ( $\text{mg g}^{-1}$ )
<b>ICG</b>	$q_{i,j,cal}$	calculated value of $q_e$ for component $i$ and measurement $j$ ( $\text{mg g}^{-1}$ )
<b>IS</b>	$q_e$	adsorbed amount at equilibrium ( $\text{mg g}^{-1}$ )
<b>RCG</b>	$q_{i,j,exp}$	experimental value of $q_e$ for component $i$ and measurement $j$ ( $\text{mg g}^{-1}$ )
<b>RMSE</b>	$r^2$	correlation coefficient
<b>SE</b>	$t$	time (h)
<b>SS</b>	$T$	temperature ( $^{\circ}\text{C}$ )
<b>UV-Vis</b>	$V$	solution volume (L)
	$x_1$	correlative constant in the extended Freundlich isotherm
<b>List of symbols</b>	$x_2$	correlative constant in the extended Freundlich isotherm
$a$	$y_1$	correlative constant in the extended Freundlich isotherm
$b$	$y_2$	correlative constant in the extended Freundlich isotherm
$C_e$	$z_1$	correlative constant in the extended Freundlich isotherm
$C_f$	$z_2$	correlative constant in the extended Freundlich isotherm
$C_{ICG}$	$z_i$	charge of ion $i$
$C_i$		
$c_i$		
$k_1$		
$k_2$		

cause leaching of bound metalloids with simultaneous contamination of runoff by these elements. Phosphorus contamination is also of concern, as it may induce eutrophication in water reservoirs in concentrations as low as  $0.02 \text{ mg L}^{-1}$  (EPA, 1995).

Iron-coated cork granulates are low-cost production materials which have been previously shown to effectively adsorb arsenic and antimony from water (Pintor et al., 2018; Pintor et al., 2020). Cork is the bark of *Quercus suber* L., a natural, renewable material (Silva et al., 2005), and coating with iron has been shown to improve its affinity toward metalloids. The use of these adsorbents has, therefore, economic and environmental advantages. However, studies so far have only assessed their suitability in single-component solutions. Accordingly, the main goal of this work was to study As, Sb, and P adsorption onto iron-coated cork granulates in binary and ternary systems.

To the authors' knowledge, this is novel research on a very common issue affecting the applicability of adsorption treatments on real-water matrices. Some studies have tackled the binary competition between As/Sb (Kolbe et al., 2011; Lan et al., 2016; Qi and Pichler, 2017; Wu et al., 2018) and As/P (Gao and Mucci, 2001; Han and Ro, 2018; Neupane et al., 2014; Niazi and Burton, 2016), but very few literature can be found on Sb/P competition or ternary As/Sb/P systems. In this study, adsorption in three binary systems (As(V)/Sb(V), As(V)/P(V) and Sb(V)/P(V)) and in ternary system (As(V)/Sb(V)/P(V)) was conducted. High initial concentrations were used, in order to obtain significant interference effects, that can be quantified for proper extrapolation to scaled-up treatment systems. The influence of other parameters, such as pH, ionic strength and electrolyte, was also investigated. The discussion and conclusions aim to approach the research gap with new considerations based on the acquired experimental data.

## 2. Materials and methods

### 2.1. Materials

Iron-coated cork granulates (ICG) were produced from raw cork granulates (RCG), provided by Corticeira Amorim, S.G.P.S. in 0.5–1.0 mm size, using the procedure previously described elsewhere (Pintor et al., 2018; Pintor et al., 2020). In short,  $20 \text{ g L}^{-1}$  RCG were contacted

with an iron oxide suspension produced from a  $0.05 \text{ mol L}^{-1}$   $\text{FeCl}_3$  solution by precipitation with NaOH at pH 7, during 24 h in a rotating shaker (Stuart, SB3) at 20 rpm. The temperature was kept at  $20.0 \pm 0.5 \text{ }^{\circ}\text{C}$  by a thermostatic cabinet. Afterwards, the granulates were washed several times and dried in an oven at  $60 \pm 1 \text{ }^{\circ}\text{C}$  overnight. The iron content was  $24 \pm 4 \text{ mg g}^{-1}$  ( $n = 13$ ) as determined by acid digestion of the adsorbents at  $150 \text{ }^{\circ}\text{C}$  followed by analysis of dissolved iron. The main characteristics of ICG adsorbent have been reported in a previous study (Pintor et al., 2018).

Contaminant solutions were prepared by dilution and/or mixture of commercial stock solutions, for As(V) and P(V) ( $1000 \pm 3 \text{ mg L}^{-1}$  of As (V) in 2–5%  $\text{HNO}_3$  (Chem-Lab) and  $10,000 \pm 40 \text{ mg L}^{-1}$  of P as  $\text{H}_3\text{PO}_4$  in 2–5%  $\text{HNO}_3$  (Chem-Lab)), and a lab-prepared stock solution of Sb(V), of  $1 \text{ g L}^{-1}$  Sb from  $\text{KSb(OH)}_6$  (Aldrich) in distilled water.

### 2.2. Analytical methods

#### 2.2.1. Arsenic and antimony

Arsenic and antimony concentrations were determined by flame atomic absorption spectroscopy (FAAS) or graphite furnace atomic absorption spectroscopy (GFAAS), depending on the concentration range.

FAAS was carried out using a GBC 932 Plus spectrometer. It was operated at a wavelength of 197.3 nm, lamp current of 5.0 mA, slit width of 1.0 nm and under nitrous oxide-acetylene flame for As and a wavelength of 217.6 nm, lamp current 5.0 mA, slit width 0.2 nm and air-acetylene flame for Sb. The measurement range was 3–50  $\text{mg L}^{-1}$  for As and 2–30  $\text{mg L}^{-1}$  for Sb.

For lower concentrations, GFAAS was used in the range 3–50  $\mu\text{g L}^{-1}$  for As and 20–100  $\mu\text{g L}^{-1}$  for Sb, using a GBC GF3000, SensAA Dual spectrometer. It was operated at similar lamp parameters as FAAS, but atomization was carried out through furnace heating in a 70 s duration program culminating at  $2000 \text{ }^{\circ}\text{C}$  for Sb and  $2400 \text{ }^{\circ}\text{C}$  for As.

#### 2.2.2. Phosphorus

Phosphorus was determined by direct colorimetry using the ascorbic acid method (Standard Methods 4500-P E (Eaton, 2005)), in the range 0–1  $\text{mg-P L}^{-1}$ . The samples were reacted with a combined reagent consisting of  $\text{H}_2\text{SO}_4$  (95%, AnalaR NORMAPUR, VWR), potassium

antimony tartrate (>99%, ACRÓS Organics), ammonium molybdate (ACS, Reag. Ph. Eur, AnalaR NORMAPUR, VWR) and ascorbic acid (AnalaR NORMAPUR, VWR). The molybdenum blue colour was used as an indicator of phosphorus concentration and measured at 880 nm in a UV-Vis spectrophotometer (UV-6300PC, VWR).

Since As(V) also forms arsenomolybdate complexes of a similar colour, a reduction was performed by adding sodium bisulfite (>99%, Sigma), followed by heating at 95 °C for 30 min, to eliminate their interference in measurement, for samples containing both P(V) and As (V). This procedure was recommended by EPA method 365.3 (US-EPA, 1978).

### 2.2.3. Iron

Iron was measured to assess the adsorbent's coating and the metal leaching during adsorption assays. FAAS was used to obtain the total Fe concentration in the range 0.1–5 mg L<sup>-1</sup>, operating at a wavelength of 248.3 nm, lamp current of 5.0 mA and slit width of 0.2 nm, under air-acetylene flame.

## 2.3. Adsorption tests

All adsorption tests were carried out in batch mode, by contacting 2.5 g L<sup>-1</sup> ICG with 45 mL solution in 50 mL polypropylene tubes, at 20 rpm in a rotating shaker, for a predetermined amount of time. The temperature was kept at 20.0 ± 0.5 °C using a thermostatic cabinet. After contact, the pH was measured and the aqueous sample was filtered through a 0.45 µm acetate cellulose filter and acidified before analysis. Adsorbed amounts ( $q$ , mg g<sup>-1</sup>) were calculated using the following mass balance equation:

$$q = \frac{V(C_i - C_f)}{m} \quad (1)$$

Where  $V$  is the solution volume (L),  $C_i$  and  $C_f$  are the initial and final concentrations of the adsorbate (mg L<sup>-1</sup>), respectively, and  $m$  is the mass of adsorbent (g).

All adsorption assays were carried out in duplicate and the results are presented with the absolute error.

### 2.3.1. Adsorption in single-component solutions

The kinetics of adsorption was studied for As(V), Sb(V) and P(V) in single-component solutions at pH 3 with an initial concentration of 25 mg L<sup>-1</sup> by performing assays with different contact times (15, 30 min, 1, 2, 4, 8, 16, 24 h, and when necessary 40 and 48 h).

Equilibrium was studied also at pH 3 by performing adsorption assays at different initial pollutant concentrations (1, 5, 10, 15, 25 and 40 mg L<sup>-1</sup>). The contact time was 24 h.

### 2.3.2. Adsorption in binary systems

The kinetics of adsorption in binary system was investigated for the three pollutant combinations (As(V)+Sb(V), As(V)+P(V), and Sb(V)+P(V)), at pH 3, with an initial concentration of each element of 25 mg L<sup>-1</sup>. The contact time was varied in the different assays (15, 30 min, 1, 2, 4, 8, 16, 24, 40 and 48 h).

Equilibrium was studied for each element, in the presence of one of the interferents at 25 mg L<sup>-1</sup>, for all six possible combinations (As(V)+Sb(V), As(V)+P(V), Sb(V)+As(V), Sb(V)+P(V), P(V)+As(V), and P(V)+Sb(V)). The target pollutant initial concentration was varied (1, 5, 10, 15, 25 and 40 mg L<sup>-1</sup>; or 5, 20, 30, 40, 50 and 60 mg L<sup>-1</sup>, in the case of P(V)+As(V)), the pH was set at 3 and the contact time at 24 h.

### 2.3.3. Adsorption in ternary system

The adsorption kinetics was also studied at pH 3, for the ternary system consisting of As(V), Sb(V) and P(V) in initial concentrations of 25 mg L<sup>-1</sup>. Contact times were 15, 30 min, 1, 2, 4, 8, 16, 24, 40 and 48 h.

The influence of pH was investigated by performing assays at pH 2, 3, 4, 5, 6, 7, 8, 9 and 10, for a contact period of 48 h. It was adjusted using adequate HNO<sub>3</sub> and NaOH solutions.

Ternary system kinetics were also acquired in the presence of KNO<sub>3</sub> electrolyte, to provide fixed ionic strength (IS) of 0.01 mol L<sup>-1</sup> and 0.1 mol L<sup>-1</sup>.

The influence of the electrolyte ions (SO<sub>4</sub><sup>2-</sup>, CO<sub>3</sub><sup>2-</sup>, Ca<sup>2+</sup>, Mg<sup>2+</sup>) was studied by varying the salt while maintaining the IS of 0.1 mol L<sup>-1</sup>. The contact time was 48 h. The salts tested were K<sub>2</sub>SO<sub>4</sub> (p.a., Merck), K<sub>2</sub>CO<sub>3</sub> (p.a., >99%, Riedel-deHaën), CaSO<sub>4</sub> \* 2 H<sub>2</sub>O (p.a., >99%, Merck) and MgSO<sub>4</sub> \* 7 H<sub>2</sub>O (>98%, PA-ACS, Panreac).

## 2.4. Equilibrium and kinetic models

### 2.4.1. Equilibrium isotherms

Equilibrium data in single-component solutions were used to fit the adsorption isotherms using the Freundlich model, according to the following equation (Freundlich, 1907):

$$q_e = K_F C_e^{1/n} \quad (3)$$

Where  $q_e$  (mg g<sup>-1</sup>) is the adsorbed amount at equilibrium with concentration  $C_e$  (mg L<sup>-1</sup>),  $K_F$  is the Freundlich equilibrium constant (mg<sup>(1-1/n)</sup> L<sup>1/n</sup> g<sup>-1</sup>) and  $n$  is a dimensionless constant related to adsorbate-adsorbent affinity. Fitting was carried out using software *CurveExpert Professional* v. 2.6.4. Langmuir fitting was also tested (Langmuir, 1918), but in most cases, the fits were poorer, so the results were not considered.

For binary systems, the extended Freundlich model was used, according to the following equations (Fritz and Schluender, 1974; Girish, 2017):

$$q_{e,1} = \frac{K_{F,1} C_{e,1} \left(\frac{1}{n_1}\right)^{+x_1}}{C_{e,1}^{x_1} + y_1 C_{e,2}^{z_1}} \quad (4)$$

$$q_{e,2} = \frac{K_{F,2} C_{e,2} \left(\frac{1}{n_2}\right)^{+x_2}}{C_{e,2}^{x_2} + y_2 C_{e,1}^{z_2}} \quad (5)$$

Where  $q_{e,1}$  and  $q_{e,2}$  are the adsorbed amounts at equilibrium (mg g<sup>-1</sup>) and  $C_{e,1}$  and  $C_{e,2}$  the equilibrium concentrations (mg L<sup>-1</sup>) of components 1 and 2;  $K_{F,1}$  and  $K_{F,2}$  are the Freundlich equilibrium constants (mg<sup>(1-1/n)</sup> L<sup>1/n</sup> g<sup>-1</sup>) and  $n_1$  and  $n_2$  the dimensionless constants related to adsorbate-adsorbent affinity of components 1 and 2 from single-component systems; and  $x_1, y_1, z_1, x_2, y_2$  and  $z_2$  are correlative constants obtained from fitting to experimental data of the binary system.

The fitting of the extended Freundlich isotherms for binary system was carried out using the Solver add-in from Microsoft Excel (Office 365), with non-linear fitting to minimize the following sum of squares (SS) function (Luo et al., 2015):

$$SS = \sum_{i=1}^2 \sum_{j=1}^{N_i} (q_{i,j,exp} - q_{i,j,cal})^2 \quad (6)$$

Where  $q_{i,j,exp}$  and  $q_{i,j,cal}$  are the experimental and calculated values of  $q_e$  for each component  $i$  and measurement  $j$ , respectively, and  $N_i$  is the number of measurements for component  $i$ .

The root mean square error (RMSE) is presented as indicative of the goodness-of-fit of the multicomponent model (Zhang et al., 2016):

$$RMSE = \sqrt{\frac{1}{N_t} SS} \quad (7)$$

Where  $N_t$  is the total number of measurements.

### 2.4.2. Kinetic models

Three empirical models were used to describe the kinetic experimental data, namely Lagergren's pseudo-first-order model (Lagergren, 1898), Ho's pseudo-second-order model (Ho, 1995) and Elovich's model (Low, 1960), as follows:

$$q = q_e(1 - \exp(-k_1 t)) \quad (8)$$

$$q = \frac{k_2 q_e^2 t}{1 + k_2 q_e t} \quad (9)$$

$$q = \frac{1}{b} \ln(1 + abt) \quad (10)$$

Where  $q$  ( $\text{mg g}^{-1}$ ) is the adsorbed amount at time  $t$  (h),  $q_e$  ( $\text{mg g}^{-1}$ ) is the adsorbed amount at equilibrium,  $k_1$  ( $\text{h}^{-1}$ ) is the pseudo-first-order kinetic constant,  $k_2$  ( $\text{g mg}^{-1} \text{h}^{-1}$ ) is the pseudo-second-order kinetic constant,  $a$  ( $\text{mg g}^{-1} \text{h}^{-1}$ ) is the initial adsorption rate, and  $b$  ( $\text{g mg}^{-1}$ ) is the reciprocal of the surface coverage when the adsorption rate is  $1/e$  of its initial value.

Fitting was also carried out using software *CurveExpert Professional v. 2.6.4*.

## 3. Results and discussion

### 3.1. Equilibrium in binary system

Equilibrium isotherms for each element in binary system were acquired for each possible combination, in order to illustrate the influence of the pollutants on each other in the removal process, and modelled using the Freundlich isotherm in single-component systems and the extended Freundlich isotherms in binary system.

Since the Freundlich model was found to be more adequate, it can be concluded that the adsorption of the pentavalent elements is a heterogeneous multilayer process.

Iron leaching was monitored during adsorption assays, and the highest recorded value of iron concentration in solution was  $2.2 \pm 0.2 \text{ mg L}^{-1}$ . This corresponded to  $0.87 \pm 0.07 \text{ mg g}^{-1}$  of iron coating lost, which is lower than 5% of the average iron content of the adsorbent. For this reason, the adsorbent was assumed to be stable at pH 3, in accordance with previous studies (Pintor et al., 2018; Pintor et al.,

2020).

The pH was also measured and was found to suffer low variation (below 0.3 pH points difference between initial and final condition) for all the experiments which were carried out at pH 3. The exception was the variation of pH experiments (Section 3.3.), and for this reason these results were expressed according to the final rather than initial pH.

#### 3.1.1. Arsenic

Equilibrium isotherms for As(V) adsorption onto ICG in single-component solution and in the presence of P(V) or Sb(V) are presented in Fig. 1. The results of Freundlich and extended Freundlich model fitting can be found in Supplementary Materials (Tables S1 and S2).

It can be observed that As(V) adsorption is decreased both by the presence of P(V) and Sb(V), although in different ways. In the case of P(V), the effect is stronger at low As(V) concentrations, while for Sb(V), hindrance of As adsorption becomes more visible as As(V) increases in solution. This difference in effect may be explained by distinct competition mechanisms occurring with P(V) and Sb(V). Like it was mentioned before, the arsenate anion is structurally more similar to phosphate than antimonate. The oxyanions of P(V) and As(V) have a tetrahedral configuration and their proton affinity constants are identical (Simeonidis et al., 2017). This chemical similarity leads to a competition for the same adsorption sites and mechanisms, namely the formation of inner-sphere complexes at the iron oxyhydroxide surface (Guo and Chen, 2005), and surface precipitation (Hongshao and Stanforth, 2001). The occurrence of surface precipitation could explain the substantial increase in As(V) adsorption with concentration, and may be the reason why the As(V) adsorption is underestimated by the multicomponent model, since it fosters multilayer adsorption (Zhang and Selim, 2008). P(V) adsorption should remain constant in this context (see Supplementary Materials, Fig. S1).

On the other hand, Sb(V) is coordinated with oxygen atoms in an octahedral structure (Simeonidis et al., 2017), leading to other adsorption mechanisms. Qi and Pichler (2017) state that although As(V) is strongly bound by specific inner-sphere interactions, Sb(V) is more weakly attached to the surface, by both outer-sphere and inner-sphere mechanisms. They suggest that As(V) is preferred to Sb(V) due to its higher negative charge and lower spatial structure; this explains why As(V) uptake is largely unaffected by Sb(V) at low concentrations.

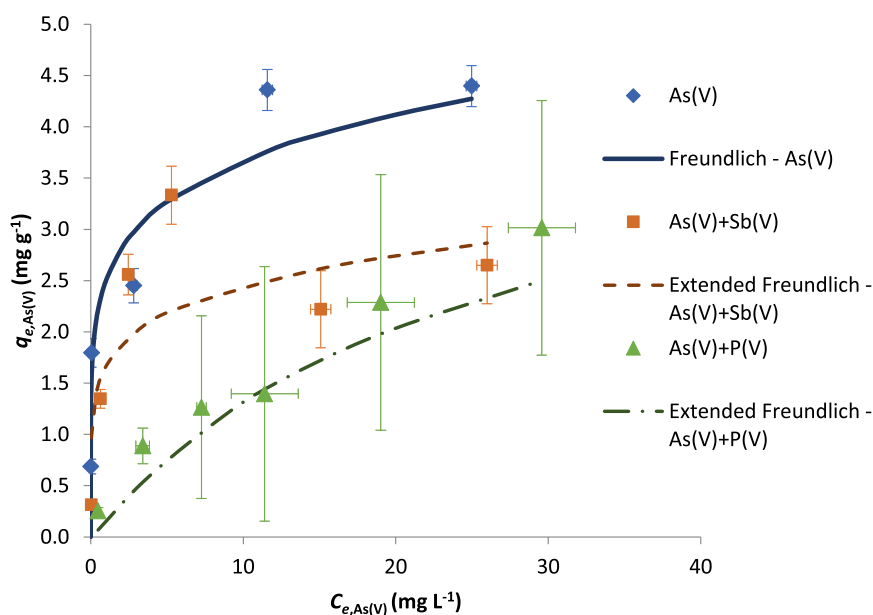


Fig. 1. As(V) adsorption onto ICG ( $C_{ICG} = 2.5 \text{ g L}^{-1}$ ; pH 3;  $T = 20.0 \pm 0.5 \text{ }^\circ\text{C}$ ; 24 h contact) in single-component solution and in the presence of Sb(V) or P(V) ( $C_i = 25 \text{ mg L}^{-1}$ ), with the fitted Freundlich and extended Freundlich isotherms.

However, at high concentrations, both As(V) and Sb(V) adsorbed amounts are reduced, with the binary model overestimating Sb(V) adsorption (see [Supplementary Materials, Fig. S1](#)). A possibility is that Sb(V), although less easily adsorbed, becomes more stable after prolonged interaction with adsorption sites, leading to their saturation, inhibiting both instant site adsorption or replacement with As(V) ([Liu et al., 2018](#)).

### 3.1.2. Antimony

The isotherms of Sb(V) adsorption in binary system, along with the one in single-component solution, are presented in [Fig. 2](#), while the values from Freundlich and extended Freundlich fitting can be found in [Supplementary Materials \(Tables S1 and S2\)](#).

The effect of As(V) and P(V) on Sb(V) uptake was similar, suggesting an analogous competitive effect. Although this effect seems to be slightly greater in the case of P(V) by looking at experimental data, the binary models predict the opposite, that is, a slightly higher inhibitory effect of As(V) compared to P(V). The model underestimates Sb(V) adsorption in the presence of As(V) but overestimates it in the presence of P(V). Theoretically, it would be expected that As(V) would compete more strongly with Sb(V) since it is more adsorbed by ICG, which is reflected in higher Freundlich parameters in single-component solution (see [Supplementary Materials, Table S1](#)). However, P(V) has a lower radius than As(V), which may facilitate its access to adsorption sites.

Previous research ([Kolbe et al., 2011](#); [Wu et al., 2018](#)) reported differences between As(V) effect on Sb(V) adsorption and the reverse. In the cited studies, while As(V) uptake remained mostly unaltered by Sb(V) presence, Sb(V) adsorption was notably suppressed in the presence of As(V). In the present work, both elements suffer interference effects ([Liu et al., 2018](#)), although despite being underestimated by the model, Sb(V) adsorption seems to be slightly more affected by As(V) than the inverse at low concentrations (see [Figs. 1–2](#)). Like it was mentioned before, As(V) may be preferred by the iron oxide surface for a variety of reasons, among them the spatial structure of the arsenate anion.

[Wu et al., \(2018\)](#) have also suggested that Sb(V) forms monodentate complexes, while As(V) (and presumably P(V)) form bidentate ones. Therefore, the latter occupy more sites and saturate the structure more easily, causing a reduction in the availability toward Sb(V), which is more weakly bound, at least in the first phases of uptake.

### 3.1.3. Phosphorus

P(V) adsorption isotherms are represented in [Fig. 3](#), in single-component and bi-component solution with As(V) or Sb(V). The results of Freundlich and extended Freundlich isotherm fitting are also found in [Supplementary Materials \(Tables S1 and S2\)](#). Unlike As(V) and Sb(V), P(V) adsorption suffered very low interference by the presence of other pnictogens, even performing better in binary solution at low equilibrium concentrations. The binary system model predicts a similar interference for both the presence of As(V) or Sb(V), underestimating P(V) adsorption, especially in the low concentration range.

Early studies on arsenate-phosphate competition for adsorption on goethite ([Hingston et al., 1971](#)) proposed the existence of common and element-specific sites. As(V) and P(V) would compete for the common sites, but not for the specific ones. Under this framework, it was observed that the proportion of P-specific sites increased with decreasing pH. Therefore, at low pH, P(V) adsorption would be less affected by competition, since it would occur mostly on element-specific sites. This is possibly valid not only for As(V) but also for Sb(V).

Moreover, [Hingston et al., \(1971\)](#) also suggest that the binary mixture may aid in opening other Fe sites for adsorption on goethite through a bridging mechanism. This may be happening here at low P(V) concentrations, where adsorption is being favoured in the presence of both As(V) or Sb(V).

### 3.2. Kinetics in binary and ternary systems

The variation in adsorption kinetics, from single, to binary, to ternary systems, for each element, is presented in [Fig. 4](#). The results of the kinetic model fitting, according to the equations presented in [Section 2.4.2.](#), can be found in [Supplementary Materials \(Table S3\)](#). The Elovich model was found to provide the best fit in most cases, confirming, along with the applicability of the Freundlich isotherm, that adsorption is heterogeneous and multilayer, with the activation energies varying with surface coverage at the binding sites ([Wang et al., 2000](#)).

Results are mostly consistent with the interferences previously observed for equilibrium studies. As(V) adsorption ([Fig. 4a](#)) was very similarly affected by Sb(V) or P(V) in binary system, which was expected considering the concentration level ([Fig. 1](#)); the rate of adsorption was slightly more affected by Sb(V) than P(V). Identically, As(V) and P(V)

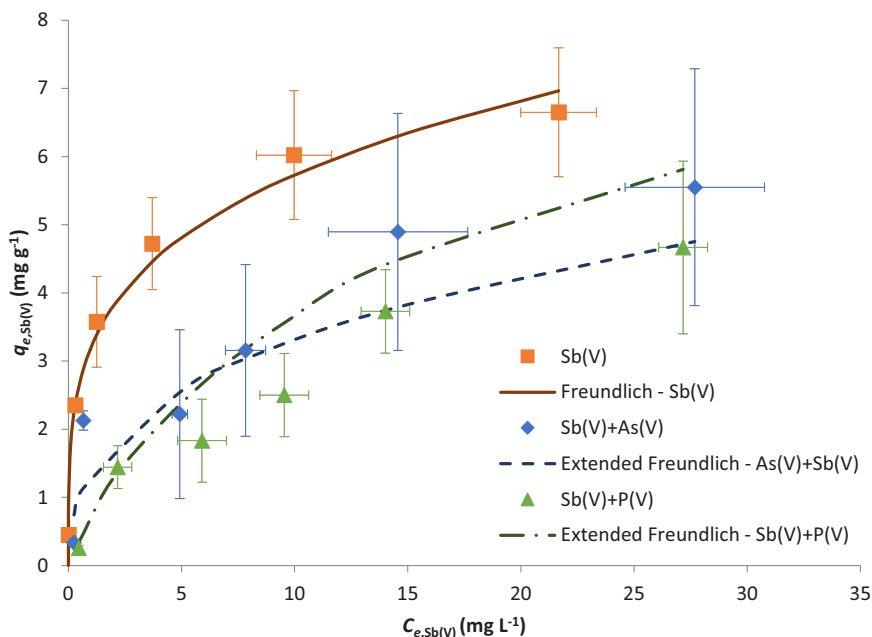


**Fig. 2.** Sb(V) adsorption onto ICG ( $C_{ICG} = 2.5 \text{ g L}^{-1}$ ; pH 3;  $T = 20.0 \pm 0.5 \text{ }^\circ\text{C}$ ; 24 h contact) in single-component solution and in the presence of As(V) or P(V) ( $C_i = 25 \text{ mg L}^{-1}$ ), with the fitted Freundlich and extended Freundlich isotherms.

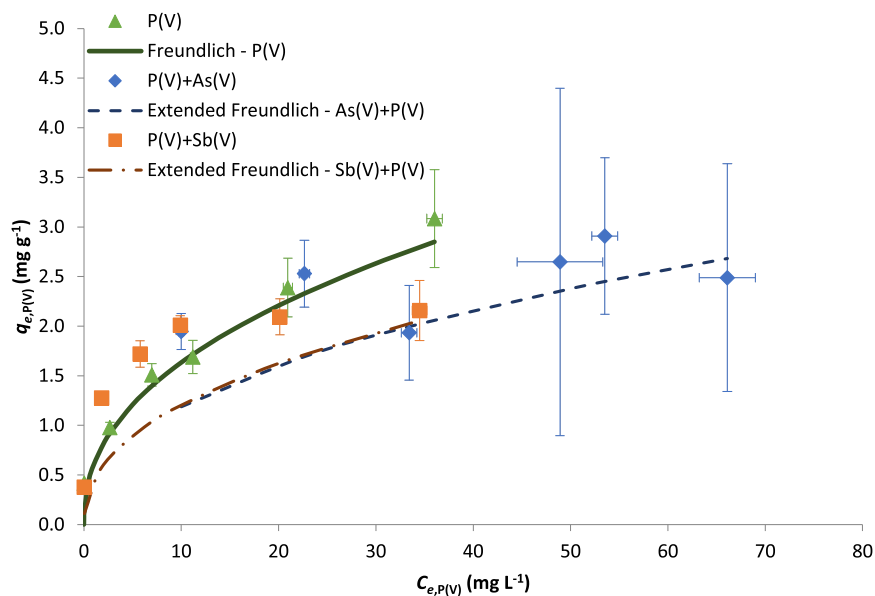


Fig. 3. P(V) adsorption onto ICG ( $C_{ICG} = 2.5 \text{ g L}^{-1}$ ; pH 3;  $T = 20.0 \pm 0.5 \text{ }^\circ\text{C}$ ; 24 h contact) in single-component solution and in the presence of As(V) or Sb(V) ( $C_i = 25 \text{ mg L}^{-1}$ ), with the fitted Freundlich and extended Freundlich isotherms.

effects on Sb(V) adsorption in binary solution were also very much alike (Fig. 4b). The adsorbed amount at equilibrium was slightly more affected by P(V), which is in accordance with the experimental results presented in Fig. 2.

Regarding P(V) adsorption, the effects of As(V) and Sb(V) on adsorption kinetics were visibly different. P(V) uptake in the presence of As(V) was fast in the first 4 h, reaching a plateau from 8 h onwards (Fig. 4c). This is consistent with a framework in which P(V) would adsorb in a fast and irreversible way on specific adsorption sites, being outcompeted by As(V) for common sites (Gao and Mucci, 2001; Hingston et al., 1971; Zhang and Selim, 2008). In the case of Sb(V), competition would occur differently since their oxyanion geometry and proton affinity vary substantially (Simeonidis et al., 2017). In both cases, the effect on adsorption capacity was higher than that presented by Fig. 3, being more in accordance with the binary model predictions.

Aggravation of interference effects in a ternary system seemed to occur for As(V) and P(V), but not Sb(V). A possible explanation resides in the fact that As(V) and P(V) are chemically analogous (Strawn, 2018), while Sb(V) presents distinct speciation, spatial structure, and binding mode, and as such interacts with the surface sites in a different way (Anson-Bertina and Klavins, 2016). Therefore, the presence of both As(V) and P(V) would not alter the chemical interferences occurring with the Sb(V) adsorption process as opposed to when only one of the elements was present. On the contrary, for As(V) and P(V), when Sb(V) is added, a new chemical interaction with possible competitive effects is introduced into the process, bringing about a novel hindrance to their uptake by the surface.

### 3.3. Effect of pH in ternary system

The effect of pH was studied in ternary system and compared with the one observed in single-component solutions, including data from previous works (Pintor et al., 2018; Pintor et al., 2020). Because the pH variation in each assay was not constant, results are presented in terms of final pH, rather than initial pH, and they can be found in Fig. 5.

Both in single-component solution and the presence of interferents, the pentavalent pnictogen adsorption tends to decrease with the increase in pH. This is a trend already widely reported for As(V), Sb(V) and P(V) adsorption from pure aqueous solutions onto iron oxides (Antelo et al., 2005; Antelo et al., 2010; Qi and Pichler, 2016; Raven et al., 1998). Since the pH of zero-charge of ICG is close to 6 (Pintor et al.,

2018), low pH contributes to the protonation of the surface, creating a positive charge that attracts the negatively charged oxyanions, while high pH promotes electrostatic repulsion between adsorbent and adsorbate and the possibility of competition with  $\text{OH}^-$  for adsorption sites (Inam et al., 2018).

Consistent with the previous studies, As(V) adsorption was the most affected by the presence of interferents over the wide range of pH, while Sb(V) and P(V) adsorption, on the other hand, were only slightly reduced. However, the pH decrease led to a sharper decrease in the adsorbed amount of Sb(V) than in those of P(V) and As(V). At lower pH, as in the rest of the studies presented in this work, Sb(V) adsorbed amount largely outweighed the other elements; however, in the neutral pH range (6–8), it decreased below As(V) and P(V) – with P(V) even becoming the most adsorbed element in ternary solution. A decrease in the preference of As(V) over P(V) with increasing pH had already been reported by other researchers (Han and Ro, 2018; Neupane et al., 2014).

Therefore, although a stark difference in the interfering behaviour is not found to be caused by pH, it is an important parameter to consider in determining which elements will be more readily uptaken by the adsorbent.

### 3.4. Effect of ionic strength in ternary system

The ionic strength (IS,  $\text{mol L}^{-1}$ ) of solutions was estimated using the following equation:

$$IS = \sum_i \frac{1}{2} c_i z_i^2 \quad (7)$$

Where  $c_i$  ( $\text{mol L}^{-1}$ ) is the concentration of ion  $i$ , and  $z_i$  its charge. Detailed calculations (found in Supplementary Materials, Table S4) estimated the IS of the ternary system of As(V), Sb(V) and P(V) at  $25 \text{ mg L}^{-1}$  in distilled water to be  $7 \times 10^{-4} \text{ mol L}^{-1}$ , or  $0.7 \text{ mmol L}^{-1}$ . The IS was then varied through the addition of  $\text{KNO}_3$  electrolyte, to provide the fixed values of 0.01 and  $0.1 \text{ mol L}^{-1}$ .

The comparison of the adsorption kinetics in ternary system at different IS, for each element, can be found in Fig. 6. The fits of the kinetic models (Eqs. (8), (9) and (10)) can be found in Supplementary Materials (Table S5).

It can be seen that ionic strength has very little effect on Sb(V) adsorption (Fig. 6b). This is consistent with previous IS studies in single-

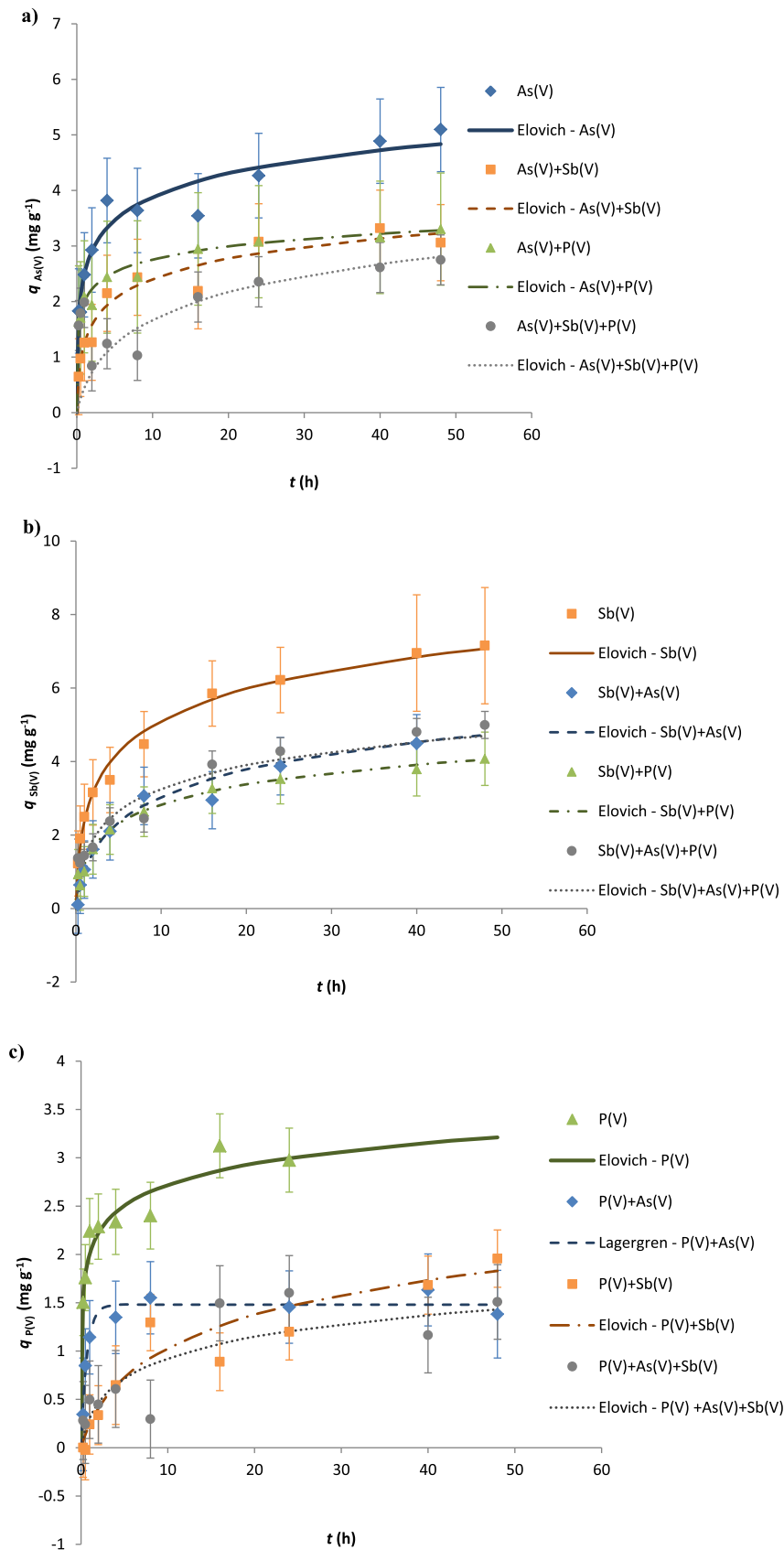


**Fig. 4.** Adsorption kinetics of a) As(V), b) Sb(V) and c) P(V) onto ICG ( $G_i = 25 \text{ mg L}^{-1}$ ;  $G_{ICG} = 2.5 \text{ g L}^{-1}$ ; pH 3;  $T = 20.0 \pm 0.5 \text{ }^\circ\text{C}$ ) in single, binary and ternary component solutions, with the best fitted kinetic models.

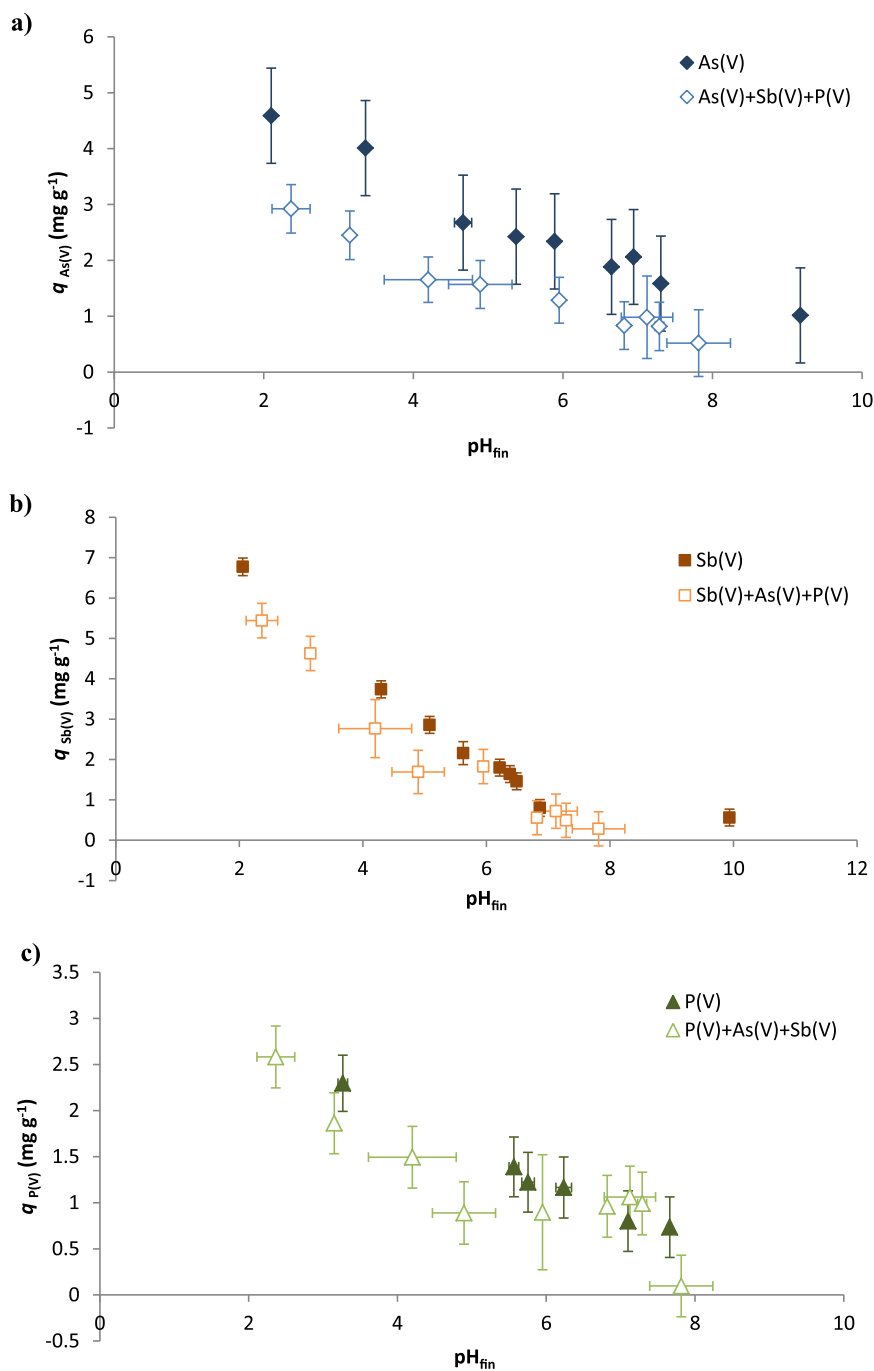
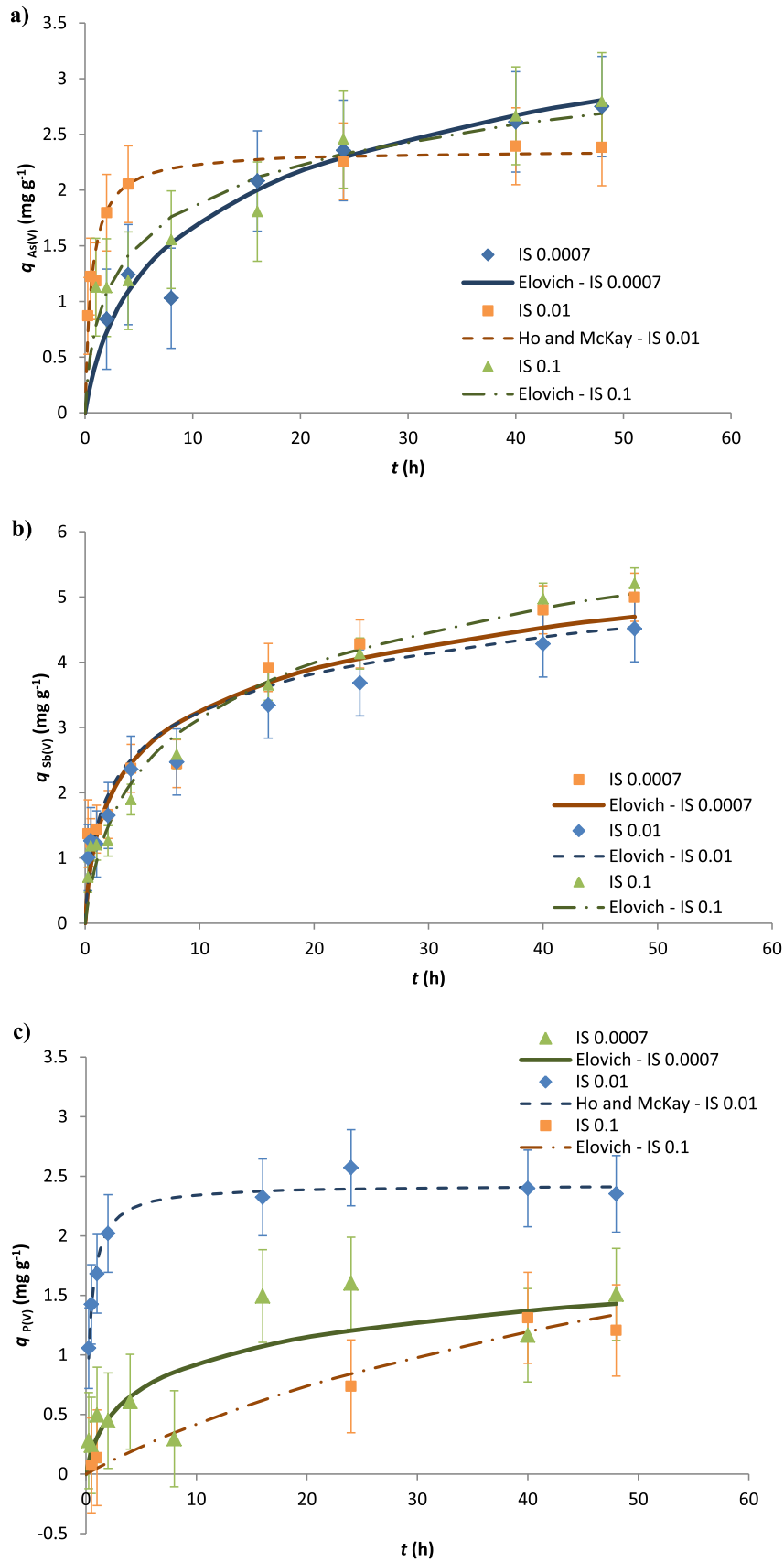


Fig. 5. Effect of pH on the adsorbed amount of a) As(V), b) Sb(V) and c) P(V) onto ICG ( $C_i = 25 \text{ mg L}^{-1}$ ;  $C_{\text{ICG}} = 2.5 \text{ g L}^{-1}$ ;  $T = 20.0 \pm 0.5 \text{ }^\circ\text{C}$ ) in single and ternary component solutions.

component Sb(V) solutions (Pintor et al., 2020). In that previous work, it was proposed that Sb(V) uptake consisted of a combination of inner-sphere and outer-sphere complexation mechanisms. From this study in ternary system, it can be advanced that the presence of As(V) and P(V), when competing for common ligand-exchange sites, probably already inhibit the outer-sphere complexation of Sb(V), so that no further competitive effect resulted from the addition of electrolyte, which binds in a non-specific manner (Xi et al., 2013).

It is a different matter for As(V) and P(V). In the case of As(V), the main effect seems to occur on the rate of adsorption, rather than the uptake capacity (Fig. 6a). It has been previously observed that an increase in IS from  $0.01$  to  $0.1 \text{ mol L}^{-1}$  can hinder the adsorption rate (Pintor et al., 2020), which was confirmed by the present results for the

three elements under study (Supplementary Materials, Table S5). For P(V), the presence of electrolyte influences both the rate and amount of adsorption (Fig. 6c). Gao and Mucci (2001) and Neupane et al., (2014) suggested that ion pair formation between  $\text{Na}^+$  and P (in a Na-based electrolyte solution) hindered phosphate adsorption in high IS conditions, causing an increased preference for As(V). A similar mechanism, but with the  $\text{K}^+$  electrolyte, could explain the present results for  $0.1 \text{ mol L}^{-1}$  IS, where P(V) adsorption is decreased. However, the same effect does not seem to hold at  $0.01 \text{ mol L}^{-1}$  IS, where P(V) adsorption is increased from the baseline, in the absence of electrolyte. In this case, another explanation may be found in a study by Han and Ro (2018), which reports an interesting trend caused by the increase of surface density in multicomponent adsorption. In their work, an absence of



**Fig. 6.** Effect of ionic strength (0.01 mol L<sup>-1</sup> and 0.1 mol L<sup>-1</sup> provided by KNO<sub>3</sub> electrolyte) on the adsorption kinetics of a) As(V), b) Sb(V) and c) P(V) onto ICG ( $C_i = 25$  mg L<sup>-1</sup>;  $C_{ICG} = 2.5$  g L<sup>-1</sup>; pH 3;  $T = 20.0 \pm 0.5$  °C) in ternary component solutions.

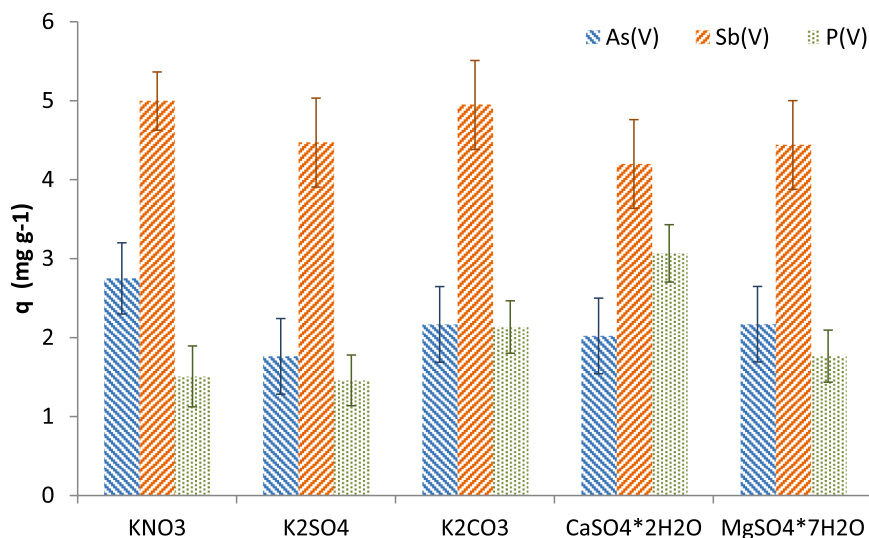


Fig. 7. Effect of the type of electrolyte ( $0.1 \text{ mol L}^{-1}$  IS) on the adsorbed amount of As(V), Sb(V) and P(V) onto ICG ( $C_i = 25 \text{ mg L}^{-1}$ ;  $C_{ICG} = 2.5 \text{ g L}^{-1}$ ; pH 3;  $T = 20.0 \pm 0.5 \text{ }^\circ\text{C}$ ) in ternary component solutions.

competitive or synergistic effects is observed for low surface density states, since saturation of adsorption sites is still far from being achieved. However, as surface coverage increases, first, a promotive effect is observed, due to a greater increase in the total adsorbed amount over the sum of individually adsorbed concentrations; only at the highest surface loading the competitive effects are strong enough to counter this effect.

Meanwhile, while As(V) and Sb(V) have been considered to be virtually unaffected by non-specific binding anions, such as nitrate, sulfate, chloride, and carbonate (Bacelo et al., 2018; Guo et al., 2007; Nagar et al., 2010; Ungureanu et al., 2017; Xi et al., 2013), P(V) is more sensitive to their presence, as various studies reported a significant reduction of its adsorption (Awual et al., 2011; Dragan et al., 2019; Pham et al., 2019; Zelmanov and Semiat, 2015). Therefore, the electrolyte itself may lead to competitive effects – in this case, between nitrates and phosphates.

In order to investigate the effect of the particular electrolyte ions in high IS conditions, the  $\text{KNO}_3$  electrolyte was substituted by  $\text{K}_2\text{SO}_4$ ,  $\text{K}_2\text{CO}_3$ ,  $\text{CaSO}_4$  or  $\text{MgSO}_4$  in the concentrations corresponding to  $0.1 \text{ mol L}^{-1}$  IS. The results for each element adsorption in ternary solution are presented in Fig. 7.

Similarly to the results in Fig. 6, it can be seen that Sb(V) is the less affected element by the variation in electrolyte ions. However, a slight reduction in adsorbed amount can be observed in the presence of sulphate as the anion. Contrary to other anions, such as  $\text{NO}_3^-$  and  $\text{CO}_3^{2-}$ , which have been shown in several studies not to affect Sb(V) adsorption, the reported effects of  $\text{SO}_4^{2-}$  have varied between synergy and competition and therefore literature is not yet conclusive on its interacting mechanism (Deng et al., 2017).

As(V) was likewise more affected by the electrolyte anion than the cation. The stronger negative charges of sulfate and carbonate caused a reduction in As(V) uptake from the first assay in the presence of nitrate. It makes sense that electrolyte anions will have a greater influence since their negative charge can disrupt the electrostatic attractions between the target oxyanions and the positively charged surface. Nevertheless, specific cations can also interfere with the process. A slight increase is observed in As(V) adsorbed amount when  $\text{Ca}^{2+}$  and  $\text{Mg}^{2+}$  are present instead of  $\text{Na}^+$ . These cations had already been reported to promote the formation of ternary complexes with As(V) and an oxide surface (Deng et al., 2018; Qiu et al., 2019).

However, the strongest effect of cations, namely  $\text{Ca}^{2+}$ , is found for P(V). Deng et al., (2018) have observed precipitation of calcium phosphate in ternary mixtures As-Ca-P. This means that increased removal of phosphate in these conditions is probably due to precipitation, and not

increased adsorption, although these microprecipitates might attach to the surface. Precipitation with Ca and Mg salts is a common technique for phosphate removal (de-Bashan and Bashan, 2004; Huang et al., 2014). P(V) adsorption also increased in the presence of the  $\text{CO}_3^{2-}$  anion, contrary to what would be expected (Bacelo et al., 2020). Since carbonate is also expected to interact by ligand-exchange with an iron oxide surface (Pepper et al., 2018), a possible explanation for the observed behaviour is an opening of Fe sites by a bridging mechanism, as previously suggested on Section 3.1.3. to occur due to the presence of As(V) and Sb(V).

#### 4. Conclusions

This work presented novel insights on the multicomponent adsorption of As(V), Sb(V) and P(V), using iron-coated cork granulates as adsorbent. Adsorption in both binary and ternary systems was assessed, in order to identify the interactions under play.

It was found that As(V) and Sb(V) were more affected by the presence of the other pnictogens than P(V). However, Sb(V) was similarly affected by both As(V) and P(V), while As(V) showed distinct adsorption behaviour whether Sb(V) or P(V) was the interferent, and aggravation of competitive effects in the presence of both. This was likely to occur due to the closer chemical similarities between As(V) and P(V) oxyanions (tetrahedral structure, identical proton affinity constants) than Sb(V) oxyanions (octahedral structure and lower negative charge).

Sb(V) adsorption was the most affected by pH variation, being strongly reduced at  $\text{pH} > 6$ . While most experimental data here presented was acquired in acidic conditions, where this element's uptake largely outweighs the others, the inverse can occur in the neutral range, where As(V) or even P(V) adsorption can predominate.

While it was less affected by As(V) or Sb(V) presence, P(V) adsorption was more sensitive to the presence of other cations and anions. In particular, the ionic strength influenced its adsorbed amount, and the addition of a Ca-based electrolyte promoted significantly increased removal (from  $1.5 \pm 0.3 \text{ mg-P g}^{-1}$  in  $\text{K}_2\text{SO}_4$  solution to  $3.1 \pm 0.4 \text{ mg-P g}^{-1}$  in  $\text{CaSO}_4$  solution), possibly by fostering a precipitation mechanism.

The observations from this study can be useful to better design adsorption treatment systems that can be robust enough to treat contaminant oxyanions, such as As(V), Sb(V) and P(V), when they are present simultaneously. This is a common occurrence in groundwaters and mining runoff and wastewater. Future work should also address the possibilities for regeneration of the adsorbent and safe end-of-life disposal.

## CRedit authorship contribution statement

**Ariana M.A. Pintor:** Conceptualization, Methodology, Formal analysis, Writing - original draft, Visualization; **Cátia C. Brandão:** Investigation; Validation; Visualization; **Rui A. R. Boaventura:** Writing - review & editing, Funding acquisition; **Cidália M. S. Botelho:** Resources, Writing - review & editing, Funding acquisition.

## Declaration of Competing Interest

The authors declare that they have no known competing financial interests or personal relationships that could have appeared to influence the work reported in this paper.

## Acknowledgements

Funding: This work is a result of: Project “AIProcMat@N2020 - Advanced Industrial Processes and Materials for a Sustainable Northern Region of Portugal 2020”, with the reference NORTE-01-0145-FEDER-000006, supported by Norte Portugal Regional Operational Programme (NORTE 2020), under the Portugal 2020 Partnership Agreement, through the European Regional Development Fund (ERDF); Associate Laboratory LSRE-LCM - UID/EQU/50020/2019 - funded by national funds through FCT/MCTES (PIDDAC). A. Pintor acknowledges her postdoctoral fellowship [SFRH/BPD/117680/2016] and her Junior Researcher contract [CEECIND/01485/2017] by FCT.

The authors kindly acknowledge Corticeira Amorim, S.G.P.S. for providing the cork granulates for this study.

## Appendix A. Supporting information

Supplementary data associated with this article can be found in the online version at [doi:10.1016/j.jhazmat.2020.124339](https://doi.org/10.1016/j.jhazmat.2020.124339).

## References

- Ansone-Bertina, L., Klavins, M., 2016. Sorption of V and VI group metalloids (As, Sb, Te) on modified peat sorbents. *Open Chem.* 14, 46–59. <https://doi.org/10.1515/chem-2016-0003>.
- Antelo, J., Avena, M., Fiol, S., López, R., Arce, F., 2005. Effects of pH and ionic strength on the adsorption of phosphate and arsenate at the goethite–water interface. *J. Colloid Interface Sci.* 285, 476–486. <https://doi.org/10.1016/j.jcis.2004.12.032>.
- Antelo, J., Fiol, S., Pérez, C., Mariño, S., Arce, F., Gondar, D., López, R., 2010. Analysis of phosphate adsorption onto ferrihydrite using the CD-MUSIC model. *J. Colloid Interface Sci.* 347, 112–119. <https://doi.org/10.1016/j.jcis.2010.03.020>.
- Awual, M.R., Jyo, A., El-Safty, S.A., Tamada, M., Seko, N., 2011. A weak-base fibrous anion exchanger effective for rapid phosphate removal from water. *J. Hazard. Mater.* 188, 164–171. <https://doi.org/10.1016/j.jhazmat.2011.01.092>.
- Bacelo, H., Pintor, A.M.A., Santos, S.C.R., Boaventura, R.A.R., Botelho, C.M.S., 2020. Performance and prospects of different adsorbents for phosphorus uptake and recovery from water. *Chem. Eng. J.* 381, 122566 <https://doi.org/10.1016/j.cej.2019.122566>.
- Bacelo, H., Vieira, B.R.C., Santos, S.C.R., Boaventura, R.A.R., Botelho, C.M.S., 2018. Recovery and valorization of tannins from a forest waste as an adsorbent for antimony uptake. *J. Clean. Prod.* 198, 1324–1335. <https://doi.org/10.1016/j.jclepro.2018.07.086>.
- Baig, S.A., Sheng, T., Hu, Y., Xu, J., Xu, X., 2015. Arsenic removal from natural water using low cost granulated adsorbents: a review. *CLEAN Soil Air Water* 43, 13–26. <https://doi.org/10.1002/clen.201200466>.
- de-Bashan, L.E., Bashan, Y., 2004. Recent advances in removing phosphorus from wastewater and its future use as fertilizer (1997–2003). *Water Res.* 38, 4222–4246. <https://doi.org/10.1016/j.watres.2004.07.014>.
- Deng, R.-J., Jin, C.-S., Ren, B.-Z., Hou, B.-L., Hursthouse, S.A., 2017. The potential for the treatment of antimony-containing wastewater by iron-based adsorbents. *Water* 9, 794. <https://doi.org/10.3390/w9100794>.
- Deng, Y., Li, Y., Li, X., Sun, Y., Ma, J., Lei, M., Weng, L., 2018. Influence of calcium and phosphate on pH dependency of arsenite and arsenate adsorption to goethite. *Chemosphere* 199, 617–624. <https://doi.org/10.1016/j.chemosphere.2018.02.018>.
- Dragan, E.S., Humelnicu, D., Dinu, M.V., 2019. Development of chitosan-poly (ethyleneimine) based double network cryogels and their application as superadsorbents for phosphate. *Carbohydr. Polym.* 210, 17–25. <https://doi.org/10.1016/j.carbpol.2019.01.054>.
- Eaton, A.D., 2005. Standard methods for the examination of water and wastewater. American Public Health Association, Baltimore, Maryland, U.S.A.

- EPA, 1995. Ecological Restoration: A Tool to Manage Stream Quality, in, Washington, D. C., pp. 168.
- Fawcett, S.E., Jamieson, H.E., Nordstrom, D.K., McCleskey, R.B., 2015. Arsenic and antimony geochemistry of mine wastes, associated waters and sediments at the Giant Mine, Yellowknife, Northwest Territories, Canada. *Appl. Geochem.* 62, 3–17. <https://doi.org/10.1016/j.apgeochem.2014.12.012>.
- Freundlich, H., 1907. Über die Adsorption in Lösungen, in: *Zeitschrift für Physikalische Chemie*, pp. 385. <https://doi.org/10.1515/zpch-1907-5723>.
- Fritz, W., Schluender, E.U., 1974. Simultaneous adsorption equilibria of organic solutes in dilute aqueous solutions on activated carbon. *Chem. Eng. Sci.* 29, 1279–1282. [https://doi.org/10.1016/0009-2509\(74\)80128-4](https://doi.org/10.1016/0009-2509(74)80128-4).
- Gao, Y., Mucci, A., 2001. Acid base reactions, phosphate and arsenate complexation, and their competitive adsorption at the surface of goethite in 0.7 M NaCl solution. *Geochim. Cosmochim. Acta* 65, 2361–2378. [https://doi.org/10.1016/S0016-7037\(01\)00589-0](https://doi.org/10.1016/S0016-7037(01)00589-0).
- Giles, D.E., Mohapatra, M., Issa, T.B., Anand, S., Singh, P., 2011. Iron and aluminium based adsorption strategies for removing arsenic from water. *J. Environ. Manag.* 92, 3011–3022. <https://doi.org/10.1016/j.jenvman.2011.07.018>.
- Girish, C.R., 2017. Various isotherm models for multicomponent adsorption: a review. *Int. J. Civ. Eng. Technol.* 8, 80–86.
- Guo, X., Chen, F., 2005. Removal of arsenic by bead cellulose loaded with iron oxyhydroxide from groundwater. *Environ. Sci. Technol.* 39, 6808–6818. <https://doi.org/10.1021/es048080k>.
- Guo, X., Du, Y., Chen, F., Park, H.-S., Xie, Y., 2007. Mechanism of removal of arsenic by bead cellulose loaded with iron oxyhydroxide ( $\beta$ -FeOOH): EXAFS study. *J. Colloid Interface Sci.* 314, 427–433. <https://doi.org/10.1016/j.jcis.2007.05.071>.
- Han, J., Ro, H.-M., 2018. Interpreting competitive adsorption of arsenate and phosphate on nanosized iron (hydr)oxides: effects of pH and surface loading. *Environ. Sci. Pollut. Res.* 25, 28572–28582. <https://doi.org/10.1007/s11356-018-2897-y>.
- Hingston, F.J., Posner, A.M., Quirk, J.P., 1971. Competitive adsorption of negatively charged ligands on oxide surfaces. *Discuss. Faraday Soc.* 52, 334–342. <https://doi.org/10.1039/DF9715200334>.
- Ho, Y.S., 1995. *Adsorption of Heavy Metals from Waste Streams by Peat*. The University of Birmingham, Birmingham, U.K.
- Hongshao, Z., Stanforth, R., 2001. Competitive adsorption of phosphate and arsenate on goethite. *Environ. Sci. Technol.* 35, 4753–4757. <https://doi.org/10.1021/es010890y>.
- Huang, H., Xiao, D., Zhang, Q., Ding, L., 2014. Removal of ammonia from landfill leachate by struvite precipitation with the use of low-cost phosphate and magnesium sources. *J. Environ. Manag.* 145, 191–198. <https://doi.org/10.1016/j.jenvman.2014.06.021>.
- Inam, M.A., Khan, R., Park, D.R., Ali, B.A., Uddin, A., Yeom, I.T., 2018. Influence of pH and contaminant redox form on the competitive removal of arsenic and antimony from aqueous media by coagulation. *Miner* 8, 574. <https://doi.org/10.3390/min8120574>.
- Kolbe, F., Weiss, H., Morgenstern, P., Wennrich, R., Lorenz, W., Schurk, K., Stanjek, H., Daus, B., 2011. Sorption of aqueous antimony and arsenic species onto akaganite. *J. Colloid Interface Sci.* 357, 460–465. <https://doi.org/10.1016/j.jcis.2011.01.095>.
- Lagergren, S.Y., 1898. Zur Theorie Der Sogenannten Adsorption Gelöster Stoffe. In: *Kunglia svenska vetenskapsakademiens handlingar*, pp. 1–39. <https://doi.org/10.1007/BF01501332>.
- Langmuir, I., 1918. The adsorption of gases on plane surfaces of glass, mica and platinum. *J. Am. Chem. Soc.* 40, 1361–1403. <https://doi.org/10.1021/ja02242a004>.
- Lan, B., Wang, Y., Wang, X., Zhou, X., Kang, Y., Li, L., 2016. Aqueous arsenic (As) and antimony (Sb) removal by potassium ferrate. *Chem. Eng. J.* 292, 389–397. <https://doi.org/10.1016/j.cej.2016.02.019>.
- Liu, B., Jian, M., Wang, H., Zhang, G., Liu, R., Zhang, X., Qu, J., 2018. Comparing adsorption of arsenic and antimony from single-solute and bi-solute aqueous systems onto ZIF-8. *Colloids Surf. A Physicochem. Eng. Asp.* 538, 164–172. <https://doi.org/10.1016/j.colsurfa.2017.10.068>.
- Low, M.J.D., 1960. Kinetics of chemisorption of gases on solids. *Chem. Rev.* 60, 267–312. <https://doi.org/10.1021/cr60205a003>.
- Luo, X., Zhang, Z., Zhou, P., Liu, Y., Ma, G., Lei, Z., 2015. Synergic adsorption of acid blue 80 and heavy metal ions (Cu<sup>2+</sup>/Ni<sup>2+</sup>) onto activated carbon and its mechanisms. *J. Ind. Eng. Chem.* 27, 164–174. <https://doi.org/10.1016/j.jiec.2014.12.031>.
- Mirza, N., Mubarak, H., Chai, L.-Y., Yong, W., Khan, M.J., Khan, Q.U., Hashmi, M.Z., Farooq, U., Sarwar, R., Yang, Z.-H., 2017. The potential use of vetiveria zizanioides for the phytoremediation of antimony, arsenic and their co-contamination. *Bull. Environ. Contam. Toxicol.* 99, 511–517. <https://doi.org/10.1007/s00128-017-2150-2>.
- Nagar, R., Sarkar, D., Makris, K.C., Datta, R., 2010. Effect of solution chemistry on arsenic sorption by Fe- and Al-based drinking-water treatment residuals. *Chemosphere* 78, 1028–1035. <https://doi.org/10.1016/j.chemosphere.2009.11.034>.
- Neupane, G., Donahoe, R.J., Arai, Y., 2014. Kinetics of competitive adsorption/desorption of arsenate and phosphate at the ferrihydrite–water interface. *Chem. Geol.* 368, 31–38. <https://doi.org/10.1016/j.chemgeo.2013.12.020>.
- Niazi, N.K., Burton, E.D., 2016. Arsenic sorption to nanoparticulate mackinawite (FeS): an examination of phosphate competition. *Environ. Pollut.* 218, 111–117. <https://doi.org/10.1016/j.envpol.2016.08.031>.
- Pepper, R.A., Couperthwaite, S.J., Millar, G.J., 2018. Re-use of waste red mud: production of a functional iron oxide adsorbent for removal of phosphorous. *J. Water Process Eng.* 25, 138–148. <https://doi.org/10.1016/j.jwpe.2018.07.006>.
- Pham, T.-H., Lee, K.-M., Kim, M.S., Seo, J., Lee, C., 2019. La-modified ZSM-5 zeolite beads for enhancement in removal and recovery of phosphate. *Microporous Mesoporous Mater.* 279, 37–44. <https://doi.org/10.1016/j.micromeso.2018.12.017>.

- Pintor, A.M.A., Vieira, B.R.C., Boaventura, R.A.R., Botelho, C.M.S., 2020. Removal of antimony from water by iron-coated cork granulates. *Sep. Purif. Technol.* 233, 116020 <https://doi.org/10.1016/j.seppur.2019.116020>.
- Pintor, A.M.A., Vieira, B.R.C., Santos, S.C.R., Boaventura, R.A.R., Botelho, C.M.S., 2018. Arsenate and arsenite adsorption onto iron-coated cork granulates. *Sci. Total Environ.* 642, 1075–1089. <https://doi.org/10.1016/j.scitotenv.2018.06.170>.
- Qiu, S., Yan, L., Jing, C., 2019. Simultaneous removal of arsenic and antimony from mining wastewater using granular TiO<sub>2</sub>: Batch and field column studies. *J. Environ. Sci.* 75, 269–276. <https://doi.org/10.1016/j.jes.2018.04.001>.
- Qi, P., Pichler, T., 2016. Sequential and simultaneous adsorption of Sb(III) and Sb(V) on ferrihydrite: implications for oxidation and competition. *Chemosphere* 145, 55–60. <https://doi.org/10.1016/j.chemosphere.2015.11.057>.
- Qi, P., Pichler, T., 2017. Competitive adsorption of As(III), As(V), Sb(III) and Sb(V) onto ferrihydrite in multi-component systems: implications for mobility and distribution. *J. Hazard. Mater.* 330, 142–148. <https://doi.org/10.1016/j.jhazmat.2017.02.016>.
- Raven, K.P., Jain, A., Loeppert, R.H., 1998. Arsenite and arsenate adsorption on ferrihydrite: kinetics, equilibrium, and adsorption envelopes. *Environ. Sci. Technol.* 32, 344–349. <https://doi.org/10.1021/es970421p>.
- Sazakli, E., Zouvelou, S.V., Kalavrouziotis, I., Leotsinidis, M., 2014. Arsenic and antimony removal from drinking water by adsorption on granular ferric oxide. *Water Sci. Technol.* 71, 622–629. <https://doi.org/10.2166/wst.2014.460>.
- Silva, S.P., Sabino, M.A., Fernandes, E.M., Correlo, V.M., Boesel, L.F., Reis, R.L., 2005. Cork: properties, capabilities and applications. *Int. Mater. Rev.* 50, 345–365. <https://doi.org/10.1179/174328005x41168>.
- Simeonidis, K., Padadopoulos, V., Tresintsi, S., Kokkinos, E., Katsoyiannis, I.A., Zouboulis, A.I., Mitrakas, M., 2017. Efficiency of iron-based oxy-hydroxides in removing antimony from groundwater to levels below the drinking water regulation limits. *Sustain* 9, 238. <https://doi.org/10.3390/su9020238>.
- Song, P., Yang, Z., Xu, H., Huang, J., Yang, X., Wang, L., 2014. Investigation of influencing factors and mechanism of antimony and arsenic removal by electrocoagulation using Fe–Al electrodes. *Ind. Eng. Chem. Res.* 53, 12911–12919. <https://doi.org/10.1021/ie501727a>.
- Strawn, D.G., 2018. Review of interactions between phosphorus and arsenic in soils from four case studies. *Geochem. Trans.* 19, 10. <https://doi.org/10.1186/s12932-018-0055-6>.
- Ungureanu, G., Santos, S., Boaventura, R., Botelho, C., 2015. Arsenic and antimony in water and wastewater: overview of removal techniques with special reference to latest advances in adsorption. *J. Environ. Manag.* 151, 326–342. <https://doi.org/10.1016/j.jenvman.2014.12.051>.
- Ungureanu, G., Santos, S.C.R., Volf, I., Boaventura, R.A.R., Botelho, C.M.S., 2017. Biosorption of antimony oxyanions by brown seaweeds: batch and column studies. *J. Environ. Chem. Eng.* 5, 3463–3471. <https://doi.org/10.1016/j.jece.2017.07.005>.
- US-EPA, 1978, Phosphorus, All Forms (Colorimetric, Ascorbic Acid, Two Reagent), in: Wang, Z., Ainsworth, C.C., Friedrich, D.M., Gassman, P.L., Joly, A.G., 2000. Kinetics and mechanism of surface reaction of salicylate on alumina in colloidal aqueous suspension. *Geochim. Cosmochim. Acta* 64, 1159–1172. [https://doi.org/10.1016/S0016-7037\(99\)00360-9](https://doi.org/10.1016/S0016-7037(99)00360-9).
- WHO, 2011. *Guidelines for drinking-water quality*. World Health Organization.
- Wu, D., Sun, S.-P., He, M., Wu, Z., Xiao, J., Chen, X.D., Wu, W.D., 2018. As(V) and Sb(V) co-adsorption onto ferrihydrite: synergistic effect of Sb(V) on As(V) under competitive conditions. *Environ. Sci. Pollut. Res.* 25, 14585–14594. <https://doi.org/10.1007/s11356-018-1488-2>.
- Xi, J., He, M., Wang, K., Zhang, G., 2013. Adsorption of antimony(III) on goethite in the presence of competitive anions. *J. Geochem. Explor.* 132, 201–208. <https://doi.org/10.1016/j.gexplo.2013.07.004>.
- Zelmanov, G., Semiat, R., 2015. The influence of competitive inorganic ions on phosphate removal from water by adsorption on iron (Fe+3) oxide/hydroxide nanoparticles-based agglomerates. *J. Water Process Eng.* 5, 143–152. <https://doi.org/10.1016/j.jwpe.2014.06.008>.
- Zhang, H., Selim, H.M., 2008. Competitive sorption-desorption kinetics of arsenate and phosphate in soils. *Soil Sci.* 173, 3–12. <https://doi.org/10.1097/ss.0b013e31815ce750>.
- Zhang, L., Wei, J., Zhao, X., Li, F., Jiang, F., Zhang, M., Cheng, X., 2016. Competitive adsorption of strontium and cobalt onto tin antimonate. *Chem. Eng. J.* 285, 679–689. <https://doi.org/10.1016/j.cej.2015.10.013>.